

# Quantification of unsteady heat transfer and phase changing process inside small icing water droplets

Cite as: Rev. Sci. Instrum. **80**, 054902 (2009); <https://doi.org/10.1063/1.3139005>  
Submitted: 13 April 2009 • Accepted: 28 April 2009 • Published Online: 21 May 2009

Zheyang Jin and Hui Hu



View Online



Export Citation

## ARTICLES YOU MAY BE INTERESTED IN

[Effect of drop size on the impact thermodynamics for supercooled large droplet in aircraft icing](#)

Physics of Fluids **28**, 062107 (2016); <https://doi.org/10.1063/1.4953411>

[Experimental investigation of the impact and freezing processes of a hot water droplet on an ice surface](#)

Physics of Fluids **31**, 057107 (2019); <https://doi.org/10.1063/1.5094691>

[Frost formation and ice adhesion on superhydrophobic surfaces](#)

Applied Physics Letters **97**, 234102 (2010); <https://doi.org/10.1063/1.3524513>



Time to get excited.  
Lock-in Amplifiers – from DC to 8.5 GHz

[Find out more](#)

 Zurich  
Instruments

# Quantification of unsteady heat transfer and phase changing process inside small icing water droplets

Zheyang Jin and Hui Hu<sup>a)</sup>

*Department of Aerospace Engineering, Iowa State University, Ames, Iowa 50011, USA*

(Received 13 April 2009; accepted 28 April 2009; published online 21 May 2009)

We report progress made in our recent effort to develop and implement a novel, lifetime-based molecular tagging thermometry (MTT) technique to quantify unsteady heat transfer and phase changing process inside small icing water droplets pertinent to wind turbine icing phenomena. The lifetime-based MTT technique was used to achieve temporally and spatially resolved temperature distribution measurements within small, convectively cooled water droplets to quantify unsteady heat transfer within the small water droplets in the course of convective cooling process. The transient behavior of phase changing process within small icing water droplets was also revealed clearly by using the MTT technique. Such measurements are highly desirable to elucidate underlying physics to improve our understanding about important microphysical phenomena pertinent to ice formation and accreting process as water droplets impinging onto wind turbine blades. © 2009 American Institute of Physics. [DOI: [10.1063/1.3139005](https://doi.org/10.1063/1.3139005)]

## I. INTRODUCTION

Wind energy is one of the cleanest renewable power sources in the world today. US Department of Energy has challenged the nation to produce 20% of its total power from wind by 2030. It has been found that the majority of wind energy potential available in US is in the northern states such as North Dakota, Kansas, South Dakota, Montana, Nebraska, Wyoming, Minnesota, and Iowa, where wind turbines are subjected to the problems caused by cold climate conditions. Wind turbine icing represents the most significant threat to the integrity of wind turbines in cold weather. It has been found that wind turbine icing would cause a variety of problems to the safe and efficient operations of wind turbines. Ice accretion on turbine blades was found to reduce the aerodynamic efficiency of wind turbines considerably, which results in wind turbine power production reduction. It has also been found that the operation of a wind turbine with an imbalance caused by ice accretion would experience an increase in the loads imposed on all turbine components, which would shorten the lifetime for wind turbine components. Uncontrolled shedding of large ice chunks from turbine blades was also found to be of special danger to service personnel as well as nearby residents, particularly when the wind power plant site borders public roads, housing, power lines, and shipping routes. In addition, icing was found to affect tower structures by increasing stresses, due to increased loads from ice accretion. This would lead to structural failures, especially when coupled to strong wind loads. Ice accretion was also found to affect the reliability of anemometers, thereby, leading to inaccurate wind speed measurements and resulting in resource estimation errors.

Advancing the technology for safe and efficient wind

turbine operation in atmospheric icing conditions requires a better understanding of the important microphysical processes pertinent to wind turbine icing phenomena. In order to elucidate underlying physics, advanced experimental techniques capable of providing accurate measurements to quantify important ice formation and accreting process, such as the unsteady heat transfer and phase changing processes inside small icing water droplets, are highly desirable. In the present study, we report progress made in our recent effort to develop and implement a novel, lifetime-based molecular tagging thermometry (MTT) technique to quantify the unsteady heat transfer and phase changing process within small icing water droplets in order to improve our understanding about the underlying physics pertinent to wind turbine icing phenomena for the development of effective and robust anti-/deicing strategies tailored for wind turbine icing mitigation.

Lifetime-based MTT technique used in the present study can be considered as an extension of the molecular tagging velocimetry and thermometry (MTV and T) technique developed by Hu and Koochesfahani.<sup>1</sup> In the sections that follow, the technical basis of the lifetime-based MTT will be described briefly along with the related properties of the phosphorescent tracer used for the MTT measurements. The application of the lifetime-based MTT technique to quantify the unsteady heat transfer and phase changing process will be given to elucidate underlying physics to improve our understanding about important microphysical phenomena pertinent to ice formation and accreting process as water droplets impinging on wind turbine blades.

## II. LIFETIME-BASED MTT TECHNIQUE

It is well known that both *fluorescence* and *phosphorescence* are molecular photoluminescence phenomena. Compared with fluorescence, which typically has a lifetime on the order of nanoseconds, phosphorescence can last as long as

<sup>a)</sup> Author to whom correspondence should be addressed. Tel.: +1-515-294-0094; FAX: 1-515-294-3262. Electronic mail: [huhui@iastate.edu](mailto:huhui@iastate.edu).

microseconds, even minutes. Since emission intensity is a function of the temperature for some substances, both fluorescence and phosphorescence of tracer molecules may be used for temperature measurements. *Laser-induced fluorescence* (LIF) techniques have been widely used for temperature measurements of liquid droplets for combustion applications.<sup>2,3</sup> *Laser-induced phosphorescence* (LIP) techniques have also been suggested recently to conduct temperature measurements of “in-flight” or levitated liquid droplets.<sup>4,5</sup> Compared with LIF techniques, the relatively long lifetime of LIP could be used to prevent interference from scattered/reflected light and any fluorescence from other substances (such as from solid surfaces) that are present in the measurement area, by simply putting a small time delay between the laser excitation pulse and the starting time for phosphorescence image acquisitions. Furthermore, LIP was found to be much more sensitive to temperature variation compared with LIF,<sup>2-6</sup> which is favorable for the accurate measurements of small temperature differences within small liquid droplets. The lifetime-based MTT technique used in the present study is a LIP-based technique.

According to quantum theory,<sup>7</sup> the intensity of a first-order photoluminescence process (either fluorescence or phosphorescence) decays exponentially. As described in Ref. 1, for a diluted solution and unsaturated laser excitation, the collected phosphorescence signal ( $S$ ) by using a gated imaging detector with integration starting at a delay time  $t_0$  after the laser pulse and a gate period of  $\delta t$  can be given by

$$S = A I_i C \varepsilon \Phi_p (1 - e^{-\delta t / \tau}) e^{-t_0 / \tau}, \quad (1)$$

where  $A$  is a parameter representing the detection collection efficiency,  $I_i$  is the local incident laser intensity,  $C$  is the concentration of the phosphorescent dye (the tagged molecular tracer),  $\varepsilon$  is the absorption coefficient, and  $\Phi_p$  is the phosphorescence quantum efficiency. The emission lifetime  $\tau$  refers to the time at which the intensity drops to 37% (i.e.,  $1/e$ ) of the initial intensity.

For an excited state, the deactivation process may involve both radiative and nonradiative pathways. The lifetime of the photoluminescence process  $\tau$  is determined by the sum of all the deactivation rates  $\tau^{-1} = k_r + k_{nr}$ , where  $k_r$  and  $k_{nr}$  are the radiative and nonradiative rate constants, respectively. According to photoluminescence kinetics,<sup>7</sup> these rate constants are, in general, temperature-dependent. The temperature dependence of the phosphorescence lifetime is the basis of the present lifetime-based MTT technique.

It should be noted that the absorption coefficient  $\varepsilon$  and quantum yield  $\Phi_p$  are also temperature-dependent in general, in addition to phosphorescence lifetime  $\tau$ , resulting in a temperature-dependent phosphorescence signal ( $S$ ). Thus, in principle, the collected phosphorescence signal ( $S$ ) may be used to measure fluid temperature if the incident laser intensity and the concentration of the phosphorescent dye remain constant (or are known) in the region of interest. It should be noted that the collected phosphorescence signal ( $S$ ) is also the function of incident laser intensity ( $I_i$ ) and the concentration of the phosphorescent dye ( $C$ ). Therefore, the spatial and temporal variations in the incident laser intensity and the nonuniformity of the phosphorescent dye (e.g., due to pho-

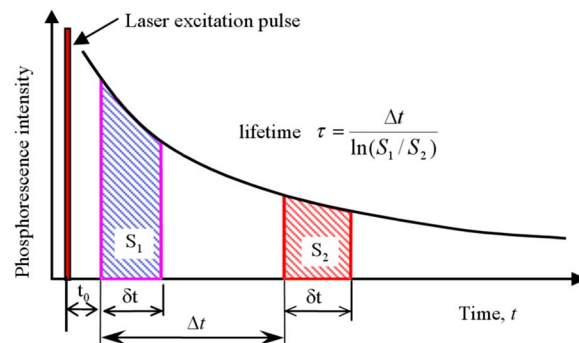


FIG. 1. (Color online) Timing chart of lifetime-based MTT technique.

toleaching) in the region of interest would have to be corrected separately in order to derive quantitative temperature data from the acquired phosphorescence images. In practice, however, it is very difficult, if not impossible, to ensure a nonvarying incident laser intensity distribution, especially for unsteady thermal phenomena with a varying index of refraction. This may cause significant error in the temperature measurements. To overcome this problem, a lifetime-based thermometry<sup>8</sup> was developed to eliminate the effects of incident laser intensity and concentration of phosphorescent dye on temperature measurements.

The lifetime-based thermometry works as follows: as illustrated in Fig. 1, LIP emission is interrogated at two successive times after the same laser excitation pulse. The first image is detected at the time  $t = t_0$  after laser excitation for a gate period  $\delta t$  to accumulate the phosphorescence intensity  $S_1$ , while the second image is detected at the time  $t = t_0 + \Delta t$  for the same gate period to accumulate the phosphorescence intensity  $S_2$ . It is easily shown,<sup>1,8</sup> using Eq. (1), that the ratio of these two phosphorescence signals ( $R$ ) is given by

$$R = S_2/S_1 = e^{-\Delta t / \tau}. \quad (2)$$

In other words, the intensity ratio of the two successive phosphorescence images ( $R$ ) is only a function of the phosphorescence lifetime  $\tau$ , and the time delay  $\Delta t$  between the image pair, which is a controllable parameter. This ratiometric approach eliminates the effects of any temporal and spatial variations in the incident laser intensity and nonuniformity of the dye concentration (e.g., due to bleaching). For a given molecular tracer and fixed  $\Delta t$  value, Eq. (2) defines a unique relation between phosphorescence intensity ratio ( $R$ ) and fluid temperature  $T$ , which can be used for thermometry.

The phosphorescent molecular tracer used for the present study is phosphorescent triplex (1-BrNp·M $\beta$ -CD·ROH). The phosphorescent triplex (1-BrNp·M $\beta$ -CD·ROH) is actually the mixture compound of three different chemicals, which are lumophore (indicated collectively by 1-BrNp), maltosyl- $\beta$ -cyclodextrin (indicated collectively by M $\beta$ -CD) and alcohols (indicated collectively by ROH). Further information about the chemical and photoluminescence properties of the phosphorescent triplex (1-BrNp·M $\beta$ -CD·ROH) is available in Refs. 9 and 10. Upon the pulsed excitation of a UV laser [quadrupled wavelength of neodymium-doped yttrium aluminum garnet (Nd:YAG) laser at 266 nm for the present study], the

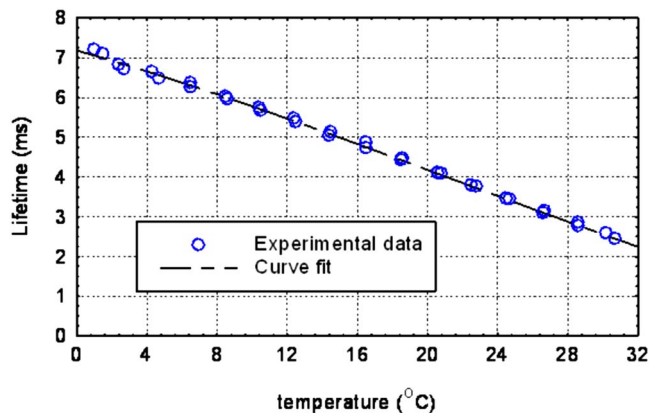


FIG. 2. (Color online) Phosphorescence lifetime vs temperature.

phosphorescence lifetime of the phosphorescent triplex (1-BrNp·M $\beta$ -CD·ROH) molecules in an aqueous solution change significantly with temperature. Figure 2 shows the measured phosphorescence lifetimes of 1-BrNp·M $\beta$ -CD·ROH molecules as a function of temperature. It can be seen clearly that phosphorescence lifetime of 1-BrNp·M $\beta$ -CD·ROH molecules varies significantly with increasing temperature, decreasing from about 7.2 to 2.5 ms as the temperature changes from 1.0 to 30.0 °C. The relative temperature sensitivity of the phosphorescence lifetime is about 3.5% per °C, which is much higher than those of fluorescent dyes.<sup>3,5,6</sup> For comparison, the temperature sensitivity of rhodamine B for LIF measurements is less than 2.0% per °C.<sup>6</sup> It is noted that, since low concentration of the phosphorescent triplex 1-BrNp·M $\beta$ -CD·ROH (on the order of  $10^{-4}M$ ) was used for the present study, the effects of the molecular tracers on the physical properties of water were believed to be negligible. During the experiments, the energy level of the pulse laser used to tag the molecular tracers within small water droplets was below 1.0 mJ/pulse. The repetition rate of the pulsed excitation was 2 Hz. The energy deposited by the excitation laser into the small water droplet was believed to be very small.

### III. EXPERIMENTAL SETUP

Figure 3 shows the schematic of the experimental setup used to implement the lifetime-based MTT technique to

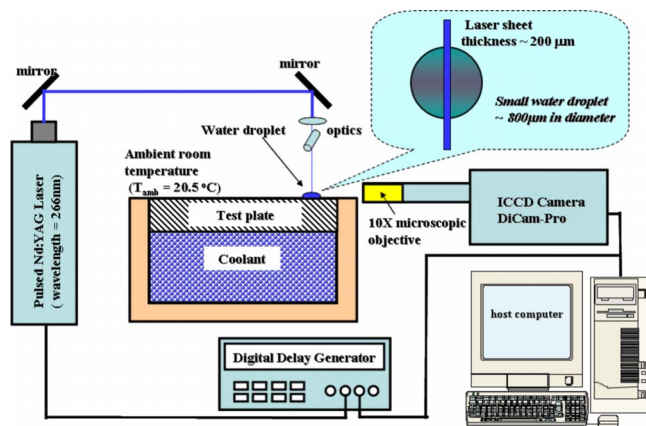


FIG. 3. (Color online) Experimental setup.

quantify unsteady heat transfer and phase changing processes within small icing water droplets. A syringe was used to generate microsized water droplets (about 400  $\mu\text{m}$  in radius and 250  $\mu\text{m}$  in height) to impinge on a test plate to simulate the processes of small water droplets impinging onto a wind turbine blade. The temperature of the test plate, which was monitored by using a thermocouple, was kept constant at a preselected low temperature level by using a water bath circulator (Neslab RTE-211). The small water droplets with initial temperature of 20.5 °C (room temperature) would be convectively cooled after they impinged onto the cold test plate. Phase changing process would occur inside the small water droplets when the temperature of the test plate was below frozen. A laser sheet ( $\sim 200$   $\mu\text{m}$  in thickness) from a pulsed Nd:YAG at a quadrupled wavelength of 266 nm was used to tag the premixed 1-BrNp·M $\beta$ -CD·ROH molecules along the middle plane of the small water droplets. A 12 bit gated intensified charge-coupled device camera (PCO DiCam-Pro, Cooke Corporation) with a fast decay phosphor (P46) was used to capture the phosphorescence emission. A 10 $\times$  microscopic objective (Mitsutoyo infinity-corrected, numerical aperture=0.28, depth of field=3.5  $\mu\text{m}$ ) was mounted in the front of the camera. The camera was operated in the dual-frame mode, where two full frame images of phosphorescence were acquired in a quick succession after the same laser excitation pulse. The camera and the pulsed Nd:YAG lasers were connected to a workstation via a digital delay generator (BNC 555 Digital Delay-Pulse Generator), which controlled the timing of the laser illumination and the image acquisition. Further details about the experimental setup and procedures to implement the lifetime-based MTT technique to quantify unsteady heat transfer and phase changing processes within small icing water droplets are available in Ref. 11.

### IV. MEASUREMENT RESULTS

Figure 4 shows a typical pair of acquired phosphorescence images for MTT measurements and the instantaneous temperature distribution inside the water droplet derived from the phosphorescence image pair. The image pair was taken at 5.0 s later after the water droplet (initial temperature 20.5 °C) impinged on the cold test plate ( $T_w=5.0$  °C). The first image [Fig. 4(a)] was acquired at 0.5 ms after the laser excitation pulse and the second image [Fig. 4(b)] at 3.5 ms after the same laser pulse with the same exposure time of 1.5 ms for the two image acquisitions. Since the time delays between the laser excitation pulse and the phosphorescence image acquisitions can eliminate scattered/reflected light and any fluorescence from other substances (such as from solid surface) in the measurement region effectively, the phosphorescence images of the water droplet are quite “clean” even though no optical filter was used for the phosphorescence image acquisition.

As described above, Eq. (2) can be used to calculate the phosphorescence lifetime of the tagged molecules on a pixel-by-pixel basis, which resulting in a distribution of the phosphorescence lifetime over a two-dimensional domain. With the calibration profile of phosphorescence lifetime versus



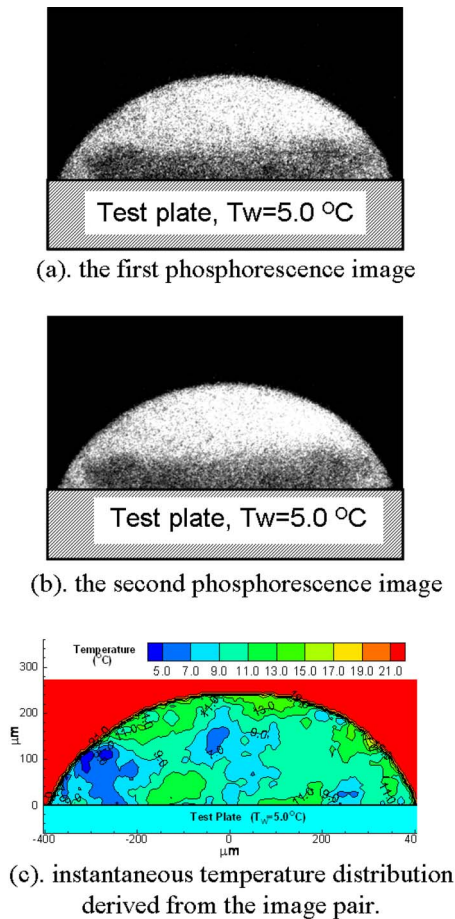


FIG. 4. (Color online) A typical MTT measurement. (a) The first phosphorescence image, (b) the second phosphorescence image, and (c) the instantaneous temperature distribution derived from the image pair.

temperature, as shown in Fig. 2, a two-dimensional, instantaneous temperature distribution within the water droplet can be derived from the phosphorescence image pair, which was shown in Fig. 4(c). Based on a time sequence of the measured transient temperature distributions within the water droplet as the one shown here, the unsteady heat transfer process within the convectively cooled water droplets was revealed quantitatively. Figure 5 shows the spatially averaged temperature of the water droplet as a function of the time after it impinged on the cold test plate, which was cal-

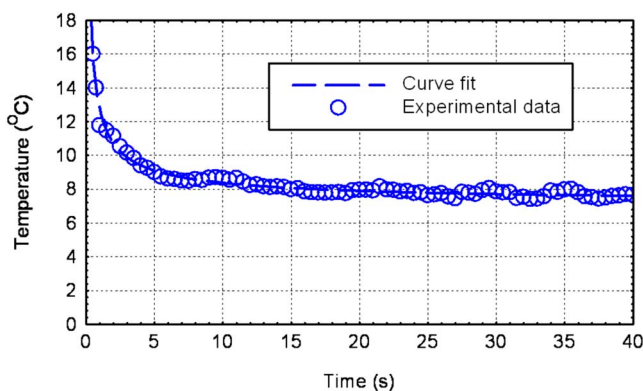


FIG. 5. (Color online) Spatially averaged temperature of the water droplet vs time.

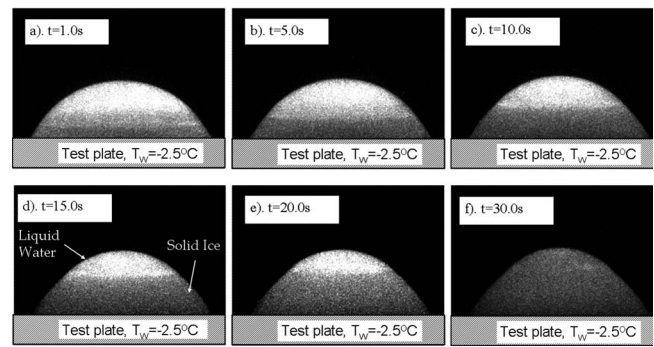


FIG. 6. The evolution of the phase changing process within a small icing water droplet.

culated based on the time sequence of measured instantaneous temperature distributions. The characteristics of the unsteady heat transfer within the water droplet in the course of convectively cooling process were revealed quantitatively from the evolution of the spatially averaged temperature of the water droplet. Since initial temperature of the water droplet ( $20.5\text{ }^{\circ}\text{C}$ ) was significantly higher than that of the cold test plate ( $T_w=5.0\text{ }^{\circ}\text{C}$ ), the temperature of the water droplet was found to decrease rapidly after it impinged on the test plate. The measurement results given in Fig. 5 also revealed that a thermal steady state would be reached at about 20 s later after the water droplet impinged on the cold test plate. The spatially averaged temperature of the water droplet would not decrease anymore when the thermal steady state was reached. It should be noted that, based on the uncertainty analysis of MTT measurements given in Ref. 1, the measurement uncertainty for the temperature data given in the present study was estimated to be within  $0.5\text{ }^{\circ}\text{C}$ .

When the temperature of the test plate was adjusted to below frozen temperature, water droplets on the test plate was found to be frozen and turned to ice crystals. Figure 6 shows the time sequence of the acquired phosphorescence images of a water droplet when it impinged onto the test plate below frozen temperature ( $T_w=-2.5\text{ }^{\circ}\text{C}$ ). The transient behavior of the phase changing process within the small icing water droplet was revealed clearly from the acquired phosphorescence images. In the images, the “brighter” region in the upper portion of the droplet represents liquid phase—water; while the “darker” region at the bottom indicates solid phase—ice. It can be seen clearly that the water droplet was round, as a cap of a sphere at the beginning. As the time goes by, the interface between the liquid phase water and solid phase ice was found to rise upward continuously, as it is expected. As a result, the droplet was found to grow upward with more and more liquid phase water turning into solid phase ice. Eventually, the spherical-cap-shaped water droplet was found to turn into a puddle-shaped ice crystal.

The required frozen time, which is defined as the time interval between the moment when a water droplet impinged on the cold test plate and the moment when the water droplet was turned into an ice crystal completely, can be determined based on the time sequence of the acquired phosphorescence images. Figure 7 shows the variations in the required frozen

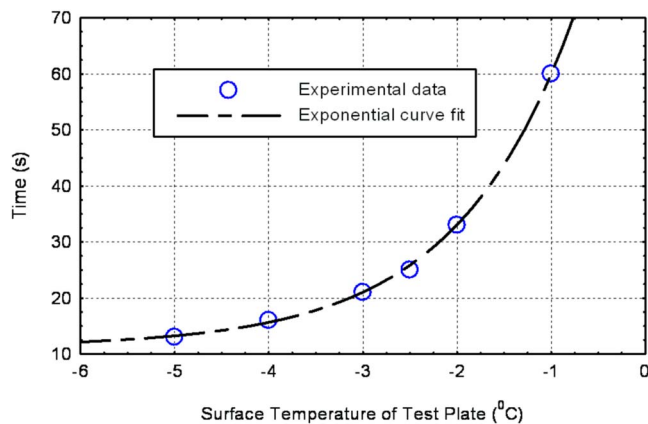


FIG. 7. (Color online) The required frozen time vs the temperature of test plate.

time of the water droplets with the surface temperature of the test plate changed from  $-1.0$  to  $-5.0$  °C. As it is expected, the required frozen time for the water droplets (initial temperature at  $20.5$  °C) turning into ice crystal was found to strongly depend on the temperature of the test plate. The required frozen time was found to decrease exponentially with the decreasing surface temperature of the test plate.

Based on the measurement results, as those shown in Figs. 4–7, important microphysical phenomena pertinent to ice formation and accreting process as water droplets impinging on wind turbine blades were revealed quantitatively. Such measurements are highly desirable to improve our understanding about the important microphysical processes pertinent to wind turbine icing phenomena in order to explore effective and robust anti-/deicing strategies tailored for wind turbine icing mitigation to ensure safer and more efficient operation of wind turbines in cold weather.

## V. CONCLUSION

A lifetime-based MTT technique was developed and implemented to quantify unsteady heat transfer and phase changing process inside small icing water droplets pertinent to wind turbine icing phenomena. For MTT measurements, a pulsed laser is used to “tag” phosphorescent molecules pre-

mixed within small water droplets. Long-lived laser-induced phosphorescence is imaged at two successive times after the same laser excitation pulse. The temperature measurement is achieved by taking advantage of the temperature dependence of phosphorescence lifetime, which is estimated from the intensity ratio of the acquired phosphorescence image pair. The lifetime-based MTT technique was used to achieve temporally and spatially resolved temperature distribution measurements within small, convectively cooled water droplets to quantify unsteady heat transfer within the small water droplets in the course of convective cooling process. Time evolution of phase changing process within small icing water droplets was also revealed clearly. Such measurements are highly desirable to elucidate underlying physics to improve our understanding about important microphysical processes pertinent to wind turbine icing phenomena for safer and more efficient operation of wind turbines in cold weather.

## ACKNOWLEDGMENTS

The authors want to thank Dr. M. M. Koochesfahani of Michigan State University for providing chemicals used for the present study. The support of National Science Foundation CAREER program under Award No. CTS-0545918 is gratefully acknowledged.

- <sup>1</sup>H. Hu and M. Koochesfahani, *Meas. Sci. Technol.* **17**, 1269 (2006).
- <sup>2</sup>Q. Lu and A. Melton, *AIAA J.* **38**, 95 (2000).
- <sup>3</sup>M. Wolff, A. Delconte, F. Schmidt, P. Gucher, and F. Lemoine, *Meas. Sci. Technol.* **18**, 697 (2007).
- <sup>4</sup>A. Omrane, G. Juhlin, F. Ossler, and M. Alden, *Appl. Opt.* **43**, 3523 (2004).
- <sup>5</sup>A. Omrane, S. Santesson, M. Alden, and S. Nilsson, *Lab Chip* **4**, 287 (2004).
- <sup>6</sup>H. Hu, C. Lum, and M. Koochesfahani, *Exp. Fluids* **40**, 753 (2006).
- <sup>7</sup>P. Pringsheim, *Fluorescence and Phosphorescence* (Interscience, New York, 1949).
- <sup>8</sup>H. Hu and M. M. Koochesfahani, *J. Visualization* **6** (2), 143 (2003).
- <sup>9</sup>W. K. Hartmann, M. H. B. Gray, A. Ponce, and D. G. Nocera, *Inorg. Chim. Acta* **243**, 239 (1996).
- <sup>10</sup>M. M. Koochesfahani and D. G. Nocera, in *Handbook of Experimental Fluid Dynamics*, edited by J. Foss, C. Tropea, and A. Yarin (Springer, Berlin, 2007), Chap. 5.4.
- <sup>11</sup>Z. Jin, “Experimental Investigations of Micro-Scale Thermal Flow Phenomena by Using Advanced Flow Diagnostic Techniques,” Ph.D. thesis, Iowa State University, 2008.